Landau-Zener model: Effects of finite coupling duration

N. V. Vitanov [1,2] and B. M. Garraway [1]

[1] *Optics Section, Blackett Laboratory, Imperial College, Prince Consort Road, London SW7 2BZ, United Kingdom*
[2] *Research Institute for Theoretical Physics, P.O. Box 9 (Siltavuorenpenger 20 C), University of Helsinki, 00014 Helsinki, Finland*
(Received 11 January 1996)

We present the generalization of the Landau-Zener model for a constant coupling of a *finite* duration. The exact evolution matrix is expressed in terms of sums of by-products of parabolic cylinder functions estimated at the turn-on time and at the turn-off time of the coupling. Various approximations in terms of simpler functions are derived and applied to several physically distinct cases. They allow us to study the dependence of the transition probability on the interaction parameters: coupling strength, coupling duration, and detuning slope. Furthermore, the analytic approximations reveal the effects of the finite coupling duration as well as those caused by adding a constant detuning shift, absence of a level crossing, turn-on time *or* turn-off time near the crossing (''half crossing''), turn-on time *and* turn-off time near the crossing (''nonsubstantial crossing''). The results are used to obtain analytic approximations to the time evolution in the original Landau-Zener model. Furthermore, following related studies on other models, we define the Landau-Zener *class* of models that, along with the finite Landau-Zener model presented in this work, contains an infinite number of members that give the same transition probability. Comparison of this class to the Allen-Eberly class shows that the two classes contain members with the same coupling but different detuning chirps as well as members with the same chirp but different couplings. The former case reveals chirp effects while the latter demonstrates shape effects. [S1050-2947(96)07505-1]

PACS number(s): 32.80.Bx, 33.80.Be, 42.50.−p

I. INTRODUCTION

Along with the simple Rabi solution [1], the Landau-Zener model (hereafter referred to as LZ) [2] is one of the most widely used two-state approximations in resonance physics. It is not an easy task to quote all the publications where the LZ model has been studied or used. We will only mention some recent generalizations of the original LZ model. They include accounting for relaxation [3], electron translation factors in atomic collisions studies [4], analytic approximations to the evolution matrix [5], parabolic level crossing [6], level crossing with two time scales [7], multiple level crossings [8], and three-level systems [9]. Among the experimental work, we note a recent detailed study of LZ dynamics [10].

There are several reasons for the wide usage of the LZ model. First of all, it describes the important physical case when a two-level quantum system interacting with an external field passes through resonance. Such a situation can be met in a number of areas in physics including quantum optics, atomic and molecular collisions, magnetic resonance, nuclear physics, and solid-state physics. Second, in the LZ model, the detuning is a linear function of time, which is a realistic assumption near the crossing. Third, the coupling is constant; near the crossing this is a relatively good approximation if the actual coupling changes slowly in time compared to the detuning, which is reasonably well satisfied in many cases. Fourth, the LZ model provides a very simple expression for the transition probability. Thus, as far as qualitative features are mainly concerned, the LZ model is relatively satisfactory in many cases.

When more detailed knowledge of the interaction dynamics is required, however, one finds that the LZ model suffers from two substantial defects. First, the (constant) coupling does not vanish as $t \rightarrow \pm\infty$, which implies an infinite energy, and second, the detuning, being a linear function of time, goes to infinity as $t \rightarrow \pm\infty$, which is also unphysical. These problems are insignificant when the transitions take place in a narrow time interval around the crossing and outside this region no substantial changes occur in the physically measurable quantities as the two-level system is far from resonance. Then the particular time dependences of the actual coupling and detuning far from the crossing are of no importance. When transitions can occur far from the crossing, however, the original LZ formula can fail. For instance, this is the case when the coupling is large or the detuning is small. Then, to estimate the transition probability in a particular level-crossing problem, one cannot just apply the LZ formula but should carry out more detailed calculations. An important part of the latter is the evolution around the crossing, which can still be described as a LZ problem but with a coupling of a finite duration.

In this work, we consider the generalization of the LZ model in which the coupling duration is assumed to be *finite*. We call this model *the finite Landau-Zener model*. The original LZ model is obtained as a limiting case when the turn-on and the turn-off times of the coupling approach infinity. In Sec. II, the exact evolution matrix and the transition probability are derived in terms of sums of by-products of parabolic cylinder functions evaluated at the turn-on and the turn-off times. Various approximations in terms of simpler functions are derived and discussed in Sec. III. They cover the cases when the coupling begins and/or ends far from the crossing or near the crossing. In Sec. IV, we apply our results to study the time evolution of the transition probability in the original LZ model by assuming that the turn-on time is at $-\infty$. In Sec. V, we discuss an interesting peculiarity of the two-level problem: the latter is degenerate in the sense that

53   4288   © 1996 The American Physical Society

different pairs of couplings and detunings give the same transition probability. These pairs form *classes* of models that contain an infinite number of members. The class generated by the finite Landau-Zener model is presented explicitly in Sec. V A. It contains some interesting members that allow us to make a comparison with similar pairs belonging to the Allen-Eberly class [7,11,12]. In particular, the comparison shows the effect of different coupling shapes for the same detuning chirp or the effect of different chirps for the same coupling shape. Finally, in Sec. VI, we present a summary of the results.

II. EXACT SOLUTION

The time evolution of a coherently driven two-level quantum system is described by the two coupled ordinary differential equations

$$i\frac{d}{dt}C_1(t) = -\Delta(t)C_1(t) + \Omega(t)C_2(t),$$

$$i\frac{d}{dt}C_2(t) = \Omega(t)C_1(t) + \Delta(t)C_2(t) \tag{1}$$

for the probability amplitudes $C_1(t)$ and $C_2(t)$ of states $|1\rangle$ and $|2\rangle$ where $\Omega(t) = H_{12}(t)/\hbar = H_{21}^*(t)/\hbar$ is the coupling (assumed real) between the two levels, $\Delta(t) = [H_{22}(t) - H_{11}(t)]/2\hbar$, and $H_{jk}(t) = \langle j|H(t)|k\rangle$ ($j,k=1,2$) are the Hamiltonian matrix elements. Equations (1) are obtained from the Schrödinger equation with the wave function of the two-level system written as

$$|\psi(t)\rangle = [C_1(t)|1\rangle + C_2(t)|2\rangle] e^{-(i/2\hbar)\int^t [H_{11}(t') + H_{22}(t')]dt'}.$$

Equations of the form (1) are met in a number of areas in physics including quantum optics, magnetic resonance, atomic collisions, solid state physics, etc. For example, in optics, Eqs. (1) are derived by using the rotating-wave approximation. There $2\Omega(t) = -\mathbf{d}\cdot\mathbf{E}(t)/\hbar$ is the on-resonance Rabi frequency and $2\Delta(t) = \omega_A - \omega_L$ is the atom-field detuning, where $\mathbf{d}$ is the atomic transition dipole moment, $\mathbf{E}(t)$ is the electric field of the laser pulse, ω_A is the atomic transition frequency, and ω_L is the laser frequency.

In the *original* Landau-Zener model, the coupling and the detuning are given by

$$\Omega(t) = \Omega_0, \quad \Delta(t) = \beta^2 t \tag{2}$$

and the coupling $\Omega(t)$ is supposed to last from $t \to -\infty$ to $t \to +\infty$. In the present work, we assume that it is turned on at time t_i and turned off at time t_f, that is,

$$\Omega(t) = \begin{cases} \Omega_0, & t_i \leq t \leq t_f \\ 0, & \text{anywhere else} \end{cases} \quad \Delta(t) = \beta^2 t. \tag{3}$$

Here the real constants Ω_0 and β have the dimension of frequency and will be assumed positive without loss of generality. We have chosen the slope β^2 of the detuning at the crossing $t=0$ to be positive in order to avoid unnecessary complications: the case of $\Delta(t) = -\beta^2 t$ leads to complex conjugation of the evolution matrix and change of sign of the nondiagonal elements. It turns out convenient to introduce the scaled dimensionless time

$$T = \beta t \tag{4}$$

as a new independent variable, and the scaled dimensionless coupling strength

$$\omega = \frac{\Omega_0}{\beta}. \tag{5}$$

The probability amplitudes $C_1(T_f)$ and $C_2(T_f)$ at the final time T_f are connected to their values $C_1(T_i)$ and $C_2(T_i)$ at the initial time T_i by the evolution matrix $\mathbf{U}(T_f,T_i)$:

$$a\mathbf{C}(T_f) = \mathbf{U}(T_f,T_i)\mathbf{C}(T_i), \tag{6}$$

where $\mathbf{C}(T) = [C_1(T), C_2(T)]^T$ and $T_{i,f} = \beta t_{i,f}$. As the excitation is coherent, the probability is conserved and $\mathbf{U}(T_f,T_i)$ is a unitary matrix.

To find the probability amplitudes, we decouple Eqs. (1) and obtain the following second-order equation for $C_1(T)$:

$$a\frac{d^2}{dT^2}C_1(T) + (\omega^2 + T^2 - i)C_1(T) = 0.$$

This equation is related to the Weber equation (A1) and its solution is expressed in terms of the parabolic cylinder function $D_\nu(z)$ [13,14] as

$$aC_1(T) = aD_{i\omega^2/2}(T\sqrt{2}e^{-i\pi/4}) + bD_{i\omega^2/2}(T\sqrt{2}e^{i3\pi/4}), \tag{7}$$

where a and b are constants. The solution for $C_2(T)$ can be obtained from here and Eqs. (1) using the derivative property (A2) of $D_\nu(z)$ and is

$$aC_2(T) = \frac{\omega}{\sqrt{2}}e^{-i\pi/4}[-aD_{-1+i\omega^2/2}(T\sqrt{2}e^{-i\pi/4})$$
$$+ bD_{-1+i\omega^2/2}(T\sqrt{2}e^{i3\pi/4})].$$

The constants a and b are to be found from the initial values $C_1(T_i)$ and $C_2(T_i)$ and are

$$a = \frac{\Gamma\left(1 - \frac{1}{2}i\omega^2\right)}{\sqrt{2\pi}}\left[D_{-1+i\omega^2/2}(T_i\sqrt{2}e^{i3\pi/4})C_1(T_i)\right.$$
$$\left. - \frac{\sqrt{2}}{\omega}e^{i\pi/4}D_{i\omega^2/2}(T_i\sqrt{2}e^{i3\pi/4})C_2(T_i)\right], \tag{8}$$

$$b = \frac{\Gamma\left(1 - \frac{1}{2}i\omega^2\right)}{\sqrt{2\pi}}\left[D_{-1+i\omega^2/2}(T_i\sqrt{2}e^{-i\pi/4})C_1(T_i)\right.$$
$$\left. + \frac{\sqrt{2}}{\omega}e^{i\pi/4}D_{i\omega^2/2}(T_i\sqrt{2}e^{-i\pi/4})C_2(T_i)\right], \tag{9}$$

where we have used the Wronskian relation (A3). Substituting Eqs. (8) and (9) into Eq. (7) and accounting for Eq. (6) we find the evolution matrix elements

$$U_{11}(T_f,T_i)=U_{22}^*(T_f,T_i)$$

$$=\frac{\Gamma\left(1-\frac{1}{2}i\omega^2\right)}{\sqrt{2\pi}}[D_{i\omega^2/2}(T_f\sqrt{2}e^{-i\pi/4})$$

$$\times D_{-1+i\omega^2/2}(T_i\sqrt{2}e^{i3\pi/4})$$

$$+D_{i\omega^2/2}(T_f\sqrt{2}e^{i3\pi/4})D_{-1+i\omega^2/2}$$

$$\times(T_i\sqrt{2}e^{-i\pi/4})], \tag{10}$$

$$U_{12}(T_f,T_i)=-U_{21}^*(T_f,T_i)$$

$$=\frac{\Gamma\left(1-\frac{1}{2}i\omega^2\right)}{\omega\sqrt{\pi}}e^{i\pi/4}[-D_{i\omega^2/2}(T_f\sqrt{2}e^{-i\pi/4})$$

$$\times D_{i\omega^2/2}(T_i\sqrt{2}e^{i3\pi/4})$$

$$+D_{i\omega^2/2}(T_f\sqrt{2}e^{i3\pi/4})D_{i\omega^2/2}(T_i\sqrt{2}e^{-i\pi/4})]. \tag{11}$$

Provided the atom has initially been in its ground state $|1\rangle$, that is

$$C_1(T_i)=1, \quad C_2(T_i)=0$$

the populations at time T_f are given by $P_1(T_f,T_i)=|U_{11}(T_f,T_i)|^2$, $P_2(T_f,T_i)=|U_{21}(T_f,T_i)|^2$ with $P_1(T_f,T_i)+P_2(T_f,T_i)=1$. We will only discuss $P_2(T_f,T_i)$, which represents the transition probability

$$P_2(T_f,T_i)=\frac{1}{2\sinh\frac{1}{2}\pi\omega^2}|-D_{i\omega^2/2}(T_f\sqrt{2}e^{-i\pi/4})$$

$$\times D_{i\omega^2/2}(T_i\sqrt{2}e^{i3\pi/4})+D_{i\omega^2/2}(T_f\sqrt{2}e^{i3\pi/4})$$

$$\times D_{i\omega^2/2}(T_i\sqrt{2}e^{-i\pi/4})|^2. \tag{12}$$

Equations (10)–(12) are *exact*, that is, no approximations have been made so far. The populations are expressed in terms of sums of by-products of parabolic cylinder functions. These functions can be calculated numerically by using power series, asymptotic series, or integral representations. This, however, does not represent a serious advance, compared to the direct numerical integration of Eqs. (1), in providing an insight into the interaction dynamics and the dependence of the populations on the model parameters, which is in fact the motivation for the analytical treatment. This determines the necessity of certain approximations that are considered in the next section.

III. APPROXIMATIONS TO THE TRANSITION PROBABILITY

We will derive several approximations to the transition probability that are valid when the turn-on time T_i and the turn-off time T_f of the external field are far from or near the crossing $T=0$. They are based on the asymptotic expansions of $D_\nu(z)$, suitable when T_i and T_f are large, and on the power series expansion of $D_\nu(z)$, suitable for small T_i and T_f. We consider two types of asymptotics. The *weak-coupling asymptotics* is valid when T_i and T_f are much larger than 1 and ω:

$$|T_i|,|T_f|\gg 1,\omega. \tag{13}$$

In this case we use the large-argument asymptotics of $D_\nu(z)$ given in Appendix A. The *strong-coupling asymptotics* is expected to be valid when T_i, T_f, and ω are simultaneously much larger than 1:

$$|T_i|,|T_f|,\omega\gg 1. \tag{14}$$

In this case we use the large-argument and large-order asymptotics of $D_\nu(z)$ also given in Appendix A. We also present the adiabatic-following solution [derived in Appendix B and obtained directly from Eqs. (1) without using any special functions] that is valid for large coupling:

$$\omega\gg 1.$$

We will see that the conditions of validity of the strong-coupling asymptotics are much weaker than (14): it is valid when *either* $T_{i,f}$ *or* ω are larger than 1. Thus, the strong-coupling approximation contains both the weak-coupling approximation and the adiabatic-following solution as particular cases.

It is worth discussing the physical meaning of the characteristic time scales of the problem. A scaled time equal to 1, $T=1$, means a real time $t_s=\beta^{-1}$. Mullen and co-workers [15] have shown that this is the characteristic transition time in the *sudden* limit ($\omega\ll 1$) (where, by the way, the transition probability is very small). Then the condition $|T_i|,|T_f|\gg 1$, which we call ''large time,'' means that the time intervals from the turn-on and the turn-off times to the crossing are much larger than the transition time in the sudden limit: $|t_i|,|t_f|\gg t_s$. Mullen and co-workers have also shown that the characteristic transition time in the *adiabatic* limit ($\omega\gg 1$) is given by $t_a=\omega/\beta=\Omega_0/\beta^2$. Hence, the weak-coupling condition (13) means that the turn-on and the turn-off times are much larger than the transition time in the adiabatic limit: $|t_i|,|t_f|\gg t_a$, while the strong-coupling condition (14) means that the ratio between t_i, t_f, and t_a can be arbitrary. Finally, to avoid confusion, we should stress that we adopt the term *weak coupling* to indicate that the coupling ω is small compared to $T_{i,f}$, or in other words, the actual coupling Ω_0 is small compared to the detuning $\Delta(t_{i,f})=\beta^2 t_{i,f}$ evaluated at $t_{i,f}$. In the case of *strong coupling* (which can also be called arbitrary coupling), the ratio between $T_{i,f}$ and ω, that is between Ω_0 and $\Delta(t_{i,f})=\beta^2 t_{i,f}$, can be arbitrary. Note that the latter case includes not only the actual strong coupling $\omega\gg|T_{i,f}|$ but also includes the weak coupling $\omega\ll|T_{i,f}|$ as well as the case of comparable ω and $T_{i,f}$: $\omega\approx|T_{i,f}|$.

In the finite LZ model, a universal approximation with respect to the turn-on time T_i and the turn-off time T_f is not possible. In the following subsections, we consider several cases when T_i and T_f are large or small and of the same sign or of the opposite signs. These cases, shown schematically in Fig. 1, are substantially different from a physical point of view. In Sec. III A, we study the case of a level crossing occurring in the middle of the interaction called *symmetric*
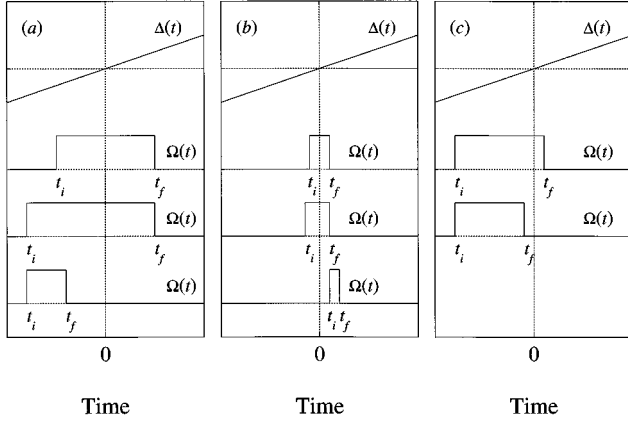
FIG. 1. The cases studied in Sec. III. (a) Substantial crossing, including symmetric crossing (top), asymmetric crossing (middle), and no crossing (bottom); (b) nonsubstantial crossing; (c) half crossing. The relation between the time t and the scaled time T used throughout the paper is $T = \beta t$.

crossing, $T_i < 0$, $T_f > 0$, $|T_i| = T_f$, both T_i and T_f being large. It is the natural generalization of the original LZ model as the latter is obtained as a particular case when $|T_i| = T_f \to \infty$. In Sec. III B, we generalize this case to unequal and large $|T_i|$ and T_f, that is $T_i < 0$, $T_f > 0$, $|T_i| \ne T_f$. This is the case of a level crossing occurring during the interaction but displaced with respect to the middle. In Sec. III C, we consider the case of T_i and T_f large but of the same sign, $T_i < 0$, $T_f < 0$. Then no level crossing occurs during the interaction. The crossing and the no-crossing cases are substantially different both from physical and from mathematical viewpoints. Physically, the transition probability in the crossing case is much larger than in the noncrossing case, which demonstrates explicitly the importance of the presence of a level crossing. Mathematically, the cases of negative and positive T_f lead to different asymptotics of the parabolic cylinder functions involved in Eqs. (10)–(12), which is a manifestation of the Stokes phenomenon [16,17]. In Sec. III D, we discuss the case when both T_i and T_f are small, which suggests using the power series expansion of $D_\nu(z)$. We call this case the ''nonsubstantial crossing'' as the transition probability does not depend on the existence of a level crossing but on the coupling duration only. In Sec. III E, we consider the case when $T_i < 0$ is large and T_f is small, that is T_f is near the crossing; this is the ''half-crossing'' case, which requires using both power series and asymptotic expansions.

A. Symmetric crossing

Let us first consider the case when the crossing point $T = 0$ is in the middle of the coupling as illustrated in the upper part of Fig. 1(a), that is $T_i = -\tau < 0$ and $T_f = \tau > 0$. The coupling duration is therefore equal to 2τ.

1. Weak-coupling asymptotics

In this case τ is much larger than both unity and the scaled coupling strength ω or, in other words, the coupling duration is larger than the transition times both in the sudden and in the adiabatic limit. The asymptotics of the transition probability is obtained from Eqs. (12), (A5), and (A6) and is

$$P_2(\tau, -\tau) \sim 1 - e^{-\pi\omega^2} - \frac{2\omega}{\tau} e^{-\pi\omega^2/2} \sqrt{1 - e^{-\pi\omega^2}} \cos\xi_w(\tau) \tag{15}$$

$$(\tau \gg 1, \omega), \tag{16}$$

where

$$\xi_w(\tau) = \frac{\omega^2}{2} \ln 2\tau^2 + \tau^2 + \frac{\pi}{4} + \arg\Gamma\left(1 - \frac{1}{2} i\omega^2\right). \tag{17}$$

2. Adiabatic-following solution

The condition for adiabatic evolution for the LZ model is [Appendix B, Eq. (B2)]

$$\frac{\omega}{2(\omega^2 + T^2)^{3/2}} \ll 1. \tag{18}$$

This condition is least satisfied at the crossing $T = 0$, when the left-hand side equals $1/(2\omega^2)$. Thus, if a crossing occurs during the interaction, as in the present case, then the adiabatic evolution requires large coupling, $\omega \gg 1$; otherwise ω may be small if $T_{i,f}$ are large enough (see Sec. III C). The adiabatic solution can be obtained from the general result (B3) derived in Appendix B and is

$$P_2(\tau, -\tau) \sim 1 - \frac{\omega^2}{\tau^2 + \omega^2} \cos^2\xi_a(\tau) \tag{19}$$

$$(\omega \gg 1), \tag{20}$$

where

$$\xi_a(\tau) = -\xi_a(-\tau) = \tau\sqrt{\tau^2 + \omega^2} + \omega^2 \ln\frac{\tau + \sqrt{\tau^2 + \omega^2}}{\omega}. \tag{21}$$

3. Strong-coupling asymptotics

In this case both τ and the scaled coupling strength ω are large, that is $\tau, \omega \gg 1$, the ratio between them being arbitrary. The asymptotics of the transition probability is obtained from Eqs. (12), (A7), and (A13) and is

$$P_2(\tau, -\tau) \sim 1 - e^{-\pi\omega^2} - e^{-\pi\omega^2/2} \sqrt{1 - e^{-\pi\omega^2}} \frac{2\tau\omega}{\tau^2 + \omega^2} \cos\xi$$

$$+ \frac{\omega^2}{\tau^2 + \omega^2} [e^{-\pi\omega^2} - (1 - e^{-\pi\omega^2})\cos^2\xi] \tag{22}$$

$$(\tau, \omega \gg 1), \tag{23}$$

where

$$\xi(\tau) = -\frac{\omega^2}{2} + \omega^2 \ln\left[\frac{1}{\sqrt{2}}(\tau + \sqrt{\tau^2 + \omega^2})\right] + \tau\sqrt{\tau^2 + \omega^2} + \frac{\pi}{4}$$

$$+ \arg\Gamma\left(1 - \frac{1}{2} i\omega^2\right). \tag{24}$$

A substantial advantage of the strong-coupling approximation (22) compared to the weak-coupling one (15) and the adiabatic solution (19) is that the strong-coupling approximation is valid in a much larger range of values of τ and ω. Indeed, it is readily verified that the strong-coupling asymptotics (22) contains the weak-coupling asymptotics (15) as a particular case in the limit $\tau \gg \omega$ and the adiabatic approximation (19) in the limit $\omega \gg 1$ [with the use of the Stirling expansion for the Γ function in (24) in the latter case]. We should point out that in the derivation of the strong-coupling approximation (22) we have not been fully consistent as we have not expanded the Γ function, which appears in the asymptotics (A13) through the connection formula (A6), by using the Stirling formula [13,14]. We have left the Γ function unexpanded in order for the strong-coupling asymptotics (22) to have the correct weak-coupling limit (15) for *any* coupling strength ω, including for small ω; otherwise the strong-coupling asymptotics would have the correct weak-coupling limit for $\tau \gg \omega \gg 1$ only, that is for large ω. On the other hand, for large ω the Γ function tends to its Stirling asymptotics anyway and keeping it unexpanded does not lead to erroneous terms. This mathematical subtlety extends considerably the range of validity of the strong-coupling expansion (22).

Evidently, both the weak-coupling asymptotics (15) and the strong-coupling asymptotics (22) reduce to the well-known LZ formula

$$P_2(+\infty, -\infty) = 1 - e^{-\pi\Lambda}, \quad \Lambda = \omega^2 = \frac{\Omega_0^2}{\beta^2} \quad (25)$$

for $\tau \to \infty$ and provide the corrections of the first order to it for τ finite. When τ increases the correction terms oscillate with amplitudes that vanish as $1/\tau$. This can be seen in Fig. 2 where the transition probability is plotted as a function of τ for two moderately small and large values of the scaled coupling strength $\omega = 0.3$ and 3. In the same figure, we have compared the approximations (15), (19), and (22) derived above to the exact values obtained by numerical integration of Eqs. (1). The adiabatic-following solution (19), which is supposed to be valid for large ω, provides a good approximation for $\omega = 3$ but fails for $\omega = 0.3$. In contrast, the weak-coupling asymptotics (15), which is supposed to be accurate for $\tau \gg 1, \omega$, is relatively good for $\omega = 0.3$ but fails completely for $\omega = 3$, even at large τ. Another defect of the weak-coupling approximation, seen in Fig. 2 for $\omega = 0.3$ and also later in Figs. 6, 7, and 9, is that it can violate unitarity and give transition probability greater than unity or negative. A more careful analysis of the weak-coupling approximation (15) leads to the conclusion that its condition of validity is more restrictive than just $\tau \gg 1, \omega$. The requirement that both $P_2(\tau, -\tau)$, given by (15), and $P_1(\tau, -\tau) = 1 - P_2(\tau, -\tau)$ should be non-negative leads to the conditions

$$\tau \gg \frac{2\omega}{\sqrt{e^{\pi\omega^2} - 1}}, 1, \quad \tau \gg 2\omega\sqrt{e^{\pi\omega^2} - 1}, 1. \quad (26)$$

The latter of these is a particularly restrictive limitation on τ even for moderate ω. This explains the inaccuracy of the weak-coupling approximation (15) for $\omega = 3$. On the other
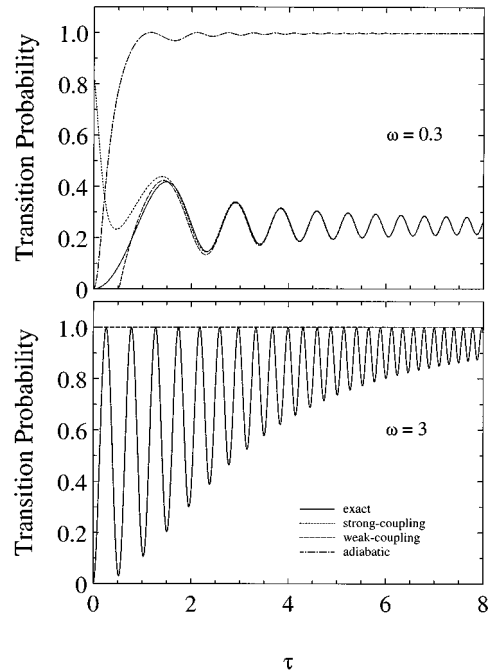
FIG. 2. The transition probability in the case of *symmetric crossing* as a function of the dimensionless parameter τ for $\omega = 0.3$ and 3. The full curves represent the exact values obtained by numerical integration of Eqs. (1), the dot-dashed curves represent the adiabatic-following solution (19), the long-line dashed curves show the weak-coupling asymptotics (15) and the short-line dashed curves show the strong-coupling asymptotics (22). For $\omega = 3$, the strong-coupling asymptotics and the adiabatic solution coincide with the exact values.

hand, Fig. 2 shows that for $\omega = 0.3$ the strong-coupling approximation (22) fits very well the numerical results for $\tau > 1$ while for $\omega = 3$ it is accurate even for $\tau < 1$. This suggests that its condition of validity is weaker than that given by Eq. (23) and is rather determined by $\tau \gg 1$ *or* $\omega \gg 1$, which is conveniently written as

$$\tau^2 + \omega^2 \gg 1. \quad (27)$$

The strong-coupling approximation can only fail when both ω and τ are small. The regions of validity of the weak-coupling asymptotics (15), the adiabatic solution (19), and the strong-coupling asymptotics (22), defined by Eqs. (26), (20), and (27), respectively, are shown in Fig. 3.

The physically interesting conclusion from Fig. 2 is that the transition probability is an oscillating function of the coupling duration 2τ with an oscillation amplitude vanishing as $1/\tau$ at large τ. The reason for these oscillations is the sudden change undergone by the system at the turn-on and the turn-off times. As τ increases, the transition probability tends to its asymptotic value determined by the LZ formula (25). Furthermore, as ω increases, the transition probability increases as well and as a result of increasing adiabaticity, it tends to unity at large ω and large enough τ, thus leading to almost complete population inversion.

The conclusions about the validity of the approximations derived above are clearly illustrated in Fig. 4 where the transition probability is plotted as a function of the scaled coupling strength ω for $\tau = 3$. The adiabatic-following solution
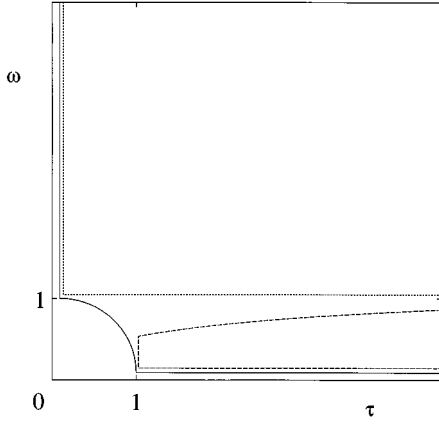
FIG. 3. Sketch of the regions of validity of various approximations in terms of the scaled dimensionless coupling strength ω and the dimensionless parameter τ equal to a half of the coupling duration. The borders of the regions of validity of the weak-coupling asymptotics (15) defined by (26) are shown by a long-line dashed curve, those of the adiabatic solution (19) defined by (20) are shown by a short-line dashed curve, and those of the strong-coupling asymptotics (22) defined by (27) are shown by a full curve.

(19) fits the exact values for $\omega > 1.5$ but is inaccurate at small ω. This is because at small ω the adiabatic condition is violated in the crossing region around $T = 0$, where nonadiabatic transitions take place. The weak-coupling asymptotics (15) is accurate for $\omega < 1$ but fails for $\omega > 1$. The strong-coupling asymptotics (22) is very accurate for any value of ω: it fits the exact values not only in the regions where the other two approximations are valid but also in the region between them and is almost indistinguishable from the exact values. The physically interesting observation from Fig. 4 is that the transition probability oscillates with an increasing amplitude
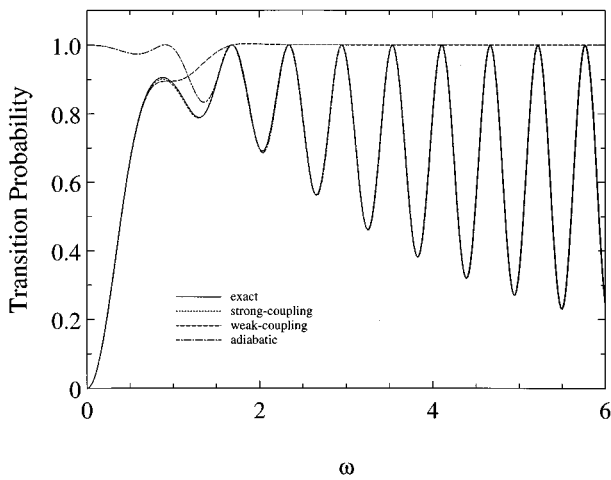
FIG. 4. The transition probability in the case of *symmetric crossing* as a function of the dimensionless coupling strength ω for $\tau = 3$. The full curve represents the exact values obtained by numerical integration of Eqs. (1), the dot-dashed curve represents the adiabatic-following solution (19), the long-line dashed curve is the weak-coupling asymptotics (15) and the short-line dashed curve is the strong-coupling asymptotics (22). The strong-coupling asymptotics is almost invisible as it nearly coincides with the exact values.

when the scaled coupling strength ω increases. The dependence of the oscillation amplitude on ω [see Eq. (22)] is the same as for a rectangular coupling of constant detuning (the so-called Rabi solution) [1]. The physical reason for this behavior is again the sudden change undergone by the system at the turn-on and the turn-off times.

B. Asymmetric crossing

Let us now consider the case when the crossing occurs during the interaction but the crossing point $T = 0$ is not in the center of the coupling as illustrated in the middle part of Fig. 1(a), that is $\tau_i \neq \tau_f$, where $T_i = -\tau_i < 0$ is the turn-on time and $T_f = \tau_f > 0$ is the turn-off time. This case is a generalization of that considered in Sec. III A to which it reduces for $\tau_i = \tau_f = \tau$. On the one hand, its comparison with the symmetric crossing demonstrates the effect of the asymmetry. On the other, a level crossing displaced from the middle of the coupling can be viewed as due to adding a constant detuning shift $\beta \delta$ to $\Delta(t)$ (3) where δ is a dimensionless parameter measuring the constant part of the detuning in units of β. In the standard LZ model adding a constant detuning does not change the populations but only generates an unimportant phase shift in the nondiagonal elements of the evolution matrix. In the finite LZ model, however, the presence of a constant detuning leads to observable changes in the interaction dynamics. If 2τ is the coupling duration, then instead of in terms of τ_i and τ_f, we can study the interaction dynamics in terms of τ and δ, parameters that may be easier to vary experimentally. The connections between these parameters are given by

$$\delta = \frac{\tau_f - \tau_i}{2}, \quad \tau = \frac{\tau_f + \tau_i}{2}, \tag{28}$$

$$\tau_i = \tau - \delta, \quad \tau_f = \tau + \delta. \tag{29}$$

1. Weak-coupling asymptotics

It is obtained from Eqs. (12), (A5), and (A6) and reads

$$P_2(\tau_f, -\tau_i) \sim 1 - e^{-\pi\omega^2} - \omega e^{-\pi\omega^2/2} \sqrt{1 - e^{-\pi\omega^2}}$$

$$\times \left[\frac{\cos \xi_w(\tau_i)}{\tau_i} + \frac{\cos \xi_w(\tau_f)}{\tau_f} \right] \tag{30}$$

$$(\tau_{i,f} \gg 1, \omega, 2\omega \sqrt{e^{\pi\omega^2} - 1}),$$

where the function $\xi_w(\tau)$ is given by Eq. (17).

2. Adiabatic-following solution

This is the regime of large coupling, $\omega \gg 1$. The solution can be obtained from the general result (B3) derived in Appendix B:

$$P_2(\tau_f, -\tau_i) \sim \frac{1}{2} + \frac{\tau_i \tau_f}{2\sqrt{(\tau_i^2 + \omega^2)(\tau_f^2 + \omega^2)}}$$

$$- \frac{\omega^2 \cos[\xi_a(\tau_f) + \xi_a(\tau_i)]}{2\sqrt{(\tau_i^2 + \omega^2)(\tau_f^2 + \omega^2)}} \qquad (31)$$

$$(\omega \gg 1),$$

where $\xi_a(\tau_{i,f})$ is given by Eq. (21).

3. Strong-coupling asymptotics

This asymptotics is obtained from Eqs. (12), (A7), and (A13) and is

$$P_2(\tau_f, -\tau_i) \sim \frac{1}{2} + \left(\frac{1}{2} - e^{-\pi\omega^2}\right) \frac{\tau_i \tau_f}{\sqrt{(\tau_i^2 + \omega^2)(\tau_f^2 + \omega^2)}} - e^{-\pi\omega^2/2}\sqrt{1 - e^{-\pi\omega^2}} \frac{\tau_i \tau_f \omega}{\sqrt{(\tau_i^2 + \omega^2)(\tau_f^2 + \omega^2)}} \left[\frac{\cos\xi(\tau_i)}{\tau_i} + \frac{\cos\xi(\tau_f)}{\tau_f}\right]$$

$$+ \frac{\omega^2\{e^{-\pi\omega^2}\cos[\xi(\tau_f) - \xi(\tau_i)] - (1 - e^{-\pi\omega^2})\cos[\xi(\tau_f) + \xi(\tau_i)]\}}{2\sqrt{(\tau_i^2 + \omega^2)(\tau_f^2 + \omega^2)}} \qquad (32)$$

$$(\tau_i^2 + \omega^2 \gg 1; \quad \tau_f^2 + \omega^2 \gg 1),$$

where $\xi(\tau)$ is given by Eq. (24). It is readily verified that the strong-coupling asymptotics (32) contains the weak-coupling asymptotics (30) as a particular case in the limit $\tau_i, \tau_f \gg \omega$ and the adiabatic approximation (31) in the limit $\omega \gg 1$.

The comparison between Eqs. (15), (19), and (22), which describe the transition probability for symmetric crossing, and Eqs. (30), (31), and (32) for asymmetric crossing shows that the asymmetry leads to more complicated oscillatory terms. For example, Fig. 5 shows that if we fix the turn-on time $T_i = -\tau_i = -10$ and vary the turn-off time τ_f, the transition probability oscillates around the value for symmetric crossing.
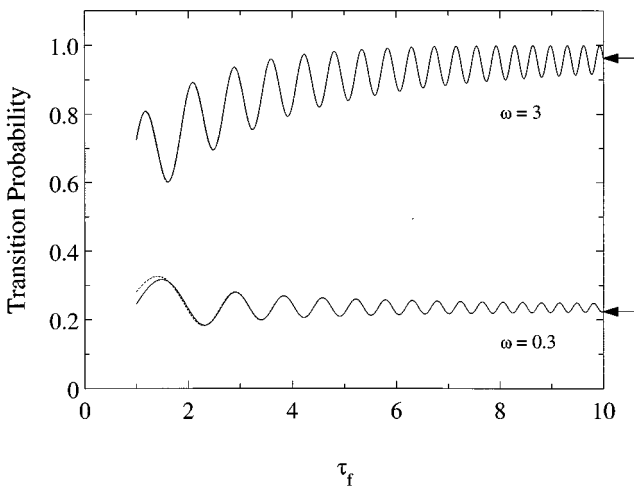
FIG. 5. The transition probability in the case of *asymmetric crossing* as a function of the dimensionless turn-off time τ_f for $T_i = -\tau_i = -10$ and two scaled coupling strengths, $\omega = 0.3$ and 3. The full curves represent the exact values obtained by numerical integration of Eqs. (1) while the dashed curves show the strong-coupling asymptotics (32), which almost coincide with the full curves. The arrows indicate the values for symmetric crossing ($\tau_i = \tau_f = 10$): $P_2 \approx 0.224$ for $\omega = 0.3$ and $P_2 \approx 0.963$ for $\omega = 3$.

In Fig. 6, we have plotted the transition probability as a function of τ (28), representing half of the coupling duration, for $\delta = 1$ and for two moderately small and large values of ω, $\omega = 0.3$ and 3. The adiabatic-following solution (31) considerably overestimates the transition probability for $\omega = 0.3$ and is not shown while for $\omega = 3$ it is very accurate and in practice, indistinguishable from the exact values. In contrast, the weak-coupling asymptotics (30) fits well the exact values for $\omega = 0.3$ but fails for $\omega = 3$. The strong-coupling asymptotics (32) is very accurate in both cases. The transition probability is seen to exhibit ''beats'' for $\omega = 0.3$, which are absent for symmetric crossing (Figs. 2 and 4). The reason for these beats is that when τ changes, τ_i and τ_f change as well [see (29)]; so do $\xi(\tau_i)$ and $\xi(\tau_f)$ in (32). For relatively large τ, where the beats are observed, the term on the second line of Eq. (32) (which is of the order of $1/\tau$) dominates the term on the third line (which is of the order of $1/\tau^2$). The former includes a sum of two cosines whose arguments $\xi(\tau_i)$ and $\xi(\tau_f)$ change in a different way when varying τ; thus, the interference between the two cosines generates the beats. Equation (32) also explains why the beats are present for $\omega = 0.3$ but not for $\omega = 3$: the oscillation amplitude is proportional to $e^{-\pi\omega^2/2}$ and thus it vanishes exponentially when ω increases.

In Fig. 7, we have plotted the transition probability as a function of the time-independent detuning shift δ (28) for two values of τ, $\tau = 3$ and 10, and for two values of ω, $\omega = 0.3$ and 3. The point $\delta = 0$ corresponds to symmetric crossing, $\tau_i = \tau_f = \tau$, while $\delta = \tau$ corresponds to half crossing, $\tau_i = 0$, $\tau_f = \tau$ (Sec. III E). Again, the adiabatic-following solution (31) is good for $\omega = 3$ (and larger) while the weak-coupling asymptotics (30) is accurate for $\omega = 0.3$ (and smaller). The strong-coupling asymptotics (32) is very accurate everywhere except near $\delta = \tau$ for $\omega = 0.3$. The reason for this inaccuracy is that for $\delta = \tau$, the turn-on time is equal to zero, $\tau_i = 0$, and the strong-coupling asymptotics at this point fails if ω is small. One can see from the figures that the transition probability generally decreases when δ increases
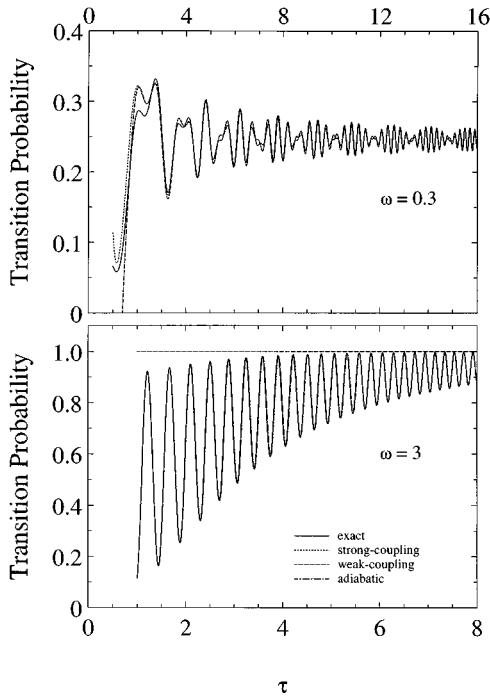
FIG. 6. The transition probability in the case of *asymmetric crossing* as a function of the dimensionless parameter $\tau = (\tau_f - \tau_i)/2$ for $\delta = 1$ and two scaled coupling strengths, $\omega = 0.3$ and 3. The full curves represent the exact values obtained by numerical integration of Eqs. (1), the dot-dashed curves represent the adiabatic-following solution (31), the long-line dashed curves show the weak-coupling asymptotics (30), and the short-line dashed curves show the strong-coupling asymptotics (32). For $\omega = 0.3$, the adiabatic solution considerably overestimates the exact values and is not shown. For $\omega = 3$, the strong-coupling asymptotics and the adiabatic solution are indiscernible from the exact values.
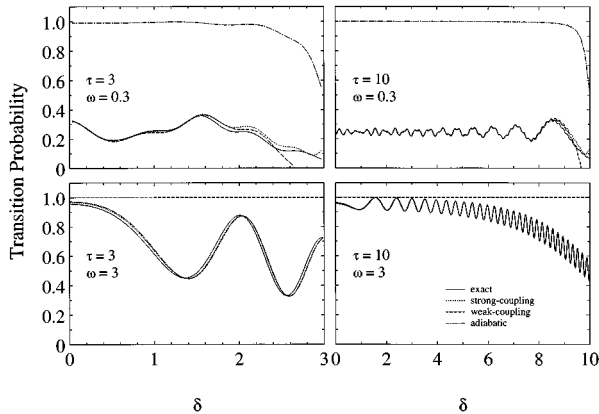
FIG. 7. The transition probability in the case of *asymmetric crossing* as a function of the time-independent dimensionless detuning shift δ for two values of the dimensionless parameter τ, $\tau = 3$ and 10, and two scaled coupling strengths, $\omega = 0.3$ and 3. The full curves represent the exact values obtained by numerical integration of Eqs. (1), the dot-dashed curves represent the adiabatic-following solution (31), the long-line dashed curves show the weak-coupling asymptotics (30) and the short-line dashed curves show the strong-coupling asymptotics (32). For $\tau = 10$ and $\omega = 3$, the strong-coupling asymptotics and the adiabatic solution are indiscernible from the exact values.

and at $\delta = \tau$ for $\omega = 3$ it tends to values near one-half, which is the asymptotic value for adiabatic excitation in the case of half crossing (Sec. III E), in contrast to the value of unity for symmetric crossing. We also conclude that the number of oscillations increases with τ, which is easy to explain by looking at the δ dependence of $\xi(\tau_{i,f})$, defined by (24) and involved in (32).

C. No crossing

A rather different situation arises when both the turn-on time and the turn-off time are situated on the same side with respect to the crossing, both being large. Without loss of generality T_i and T_f will be assumed negative, $T_i = -\tau_i < 0$, $T_f = -\tau_f < 0$ as illustrated in the lower part of Fig. 1(a). This means that no crossing occurs during the interaction, which makes this case substantially different from those considered above and from the LZ model itself.

1. Weak-coupling asymptotics

It is obtained from Eqs. (12), (A5), and (A6) and reads

$$P_2(-\tau_f, -\tau_i) \sim \frac{\omega^2}{4} \left\{ \left(\frac{1}{\tau_f} - \frac{1}{\tau_i} \right)^2 \right.$$
$$\left. + \frac{4}{\tau_f \tau_i} \sin^2 \left[\frac{\omega^2}{2} \ln \frac{\tau_f}{\tau_i} + \frac{1}{2} (\tau_f^2 - \tau_i^2) \right] \right\}$$
(33)
$$(\tau_i \gg 1, \omega; \tau_f \gg 1, \omega).$$

2. Strong-coupling asymptotics

This asymptotics is obtained from Eqs. (12), (A7), and (A13) and is

$$P_2(-\tau_f, -\tau_i) \sim \frac{1}{2} - \frac{\tau_i \tau_f}{2 \sqrt{(\tau_i^2 + \omega^2)(\tau_f^2 + \omega^2)}}$$
$$- \frac{\omega^2 \cos[\xi(\tau_f) - \xi(\tau_i)]}{2 \sqrt{(\tau_i^2 + \omega^2)(\tau_f^2 + \omega^2)}}$$
(34)
$$(\tau_i^2 + \omega^2 \gg 1; \tau_f^2 + \omega^2 \gg 1),$$

where $\xi(\tau_{i,f})$ is given by Eq. (24). The leading term (34) of the strong-coupling asymptotics has the same form as the adiabatic-following solution. This is due to the fact that when no crossing occurs the adiabatic condition (18) is easier to satisfy. For $\tau_i, \tau_f \gg \omega$ the strong-coupling asymptotics contains the weak-coupling asymptotics (33) as a particular case. The transition probability is plotted in Fig. 8 as a function of the turn-off time $T_f = -\tau_f < 0$ for a fixed turn-on time $T_i = -\tau_i = -20$ and for two values of the coupling strength: $\omega = 0.3$ and 3. It is seen that the weak-coupling asymptotics (33) is accurate for $\omega = 0.3$ even near the crossing $T = 0$, while for $\omega = 3$ it is good for large τ_f only. The strong-coupling asymptotics (34) is quite accurate for any ω including near the crossing. In contrast to the case of a crossing *during* the interaction, here the transition probability is small. This represents another clear example of the importance of level crossing in quantum physics. The useful point in the present case is that the coupling and the detuning
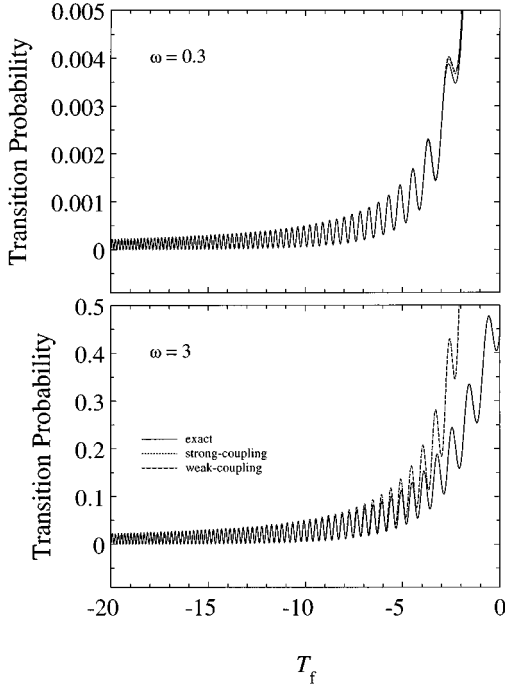
FIG. 8. The transition probability in the case of *no crossing* as a function of the dimensionless turn-off time $T_f = -\tau_f$ for $T_i = -\tau_i = -20$ and two scaled coupling strengths, $\omega = 0.3$ and 3. The full curves represent the exact values obtained by numerical integration of Eqs. (1), the long-line dashed curves show the weak-coupling asymptotics (33), and the short-line dashed curves show the strong-coupling asymptotics (34). For $\omega = 3$, the strong-coupling asymptotics is indiscernible from the exact values.

have the same time dependence in the case of crossing and no crossing; this eliminates any contribution from pulse-shape effects or different chirps. We have to note that a similar analysis for the Nikitin model has recently been carried out by one of the present authors [18].

D. Nonsubstantial crossing

Let us now consider the case when both the turn-on time T_i and the turn-off time T_f are small compared to ω^{-1} as illustrated in Fig. 1(b). Both T_i and T_f can be negative or positive. In this case one can use the power-series expansion (A4) of the parabolic cylinder functions in Eq. (12). The transition probability is small and is given by

$$P_2(T_f, T_i) = \omega^2 (T_f - T_i)^2 \left[1 - \frac{\omega^2}{3}(T_f - T_i)^2 + \cdots \right]$$

(35)

$$(\omega |T_i|, \omega |T_f| \ll 1).$$

Note that $\omega(T_f - T_i)$ is the pulse area, which is small in this case. An important observation from Eq. (35) is that up to the fourth order in T_i and T_f the transition probability depends on the coupling *duration* $T_f - T_i$ only but not on the turn-on time T_i and the turn-off time T_f separately. We should stress that the sixth-order term, which is not given for the sake of brevity, does not share this property and does depend on T_i and T_f separately, as does $P_2(T_f, T_i)$ in gen-

eral; otherwise the presence or the absence of a crossing would be of no importance, which is not the case, as we have seen above. The fact that the first term of $P_2(T_f, T_i)$ depends on $T_f - T_i$ only is not surprising because this term represents the first-order perturbation theory result, while the presence of this property in the second term is more difficult to explain and appears to be accidental. We should also stress that in the derivation of Eq. (35) no assumptions have been made about the signs of T_i and T_f, that is about the presence or the absence of a level crossing. This is because no Stokes phenomenon occurs in power series expansions in contrast to asymptotic series. From a physical point of view, the dependence of the lowest terms of $P_2(T_f, T_i)$ on the coupling duration only, irrespective of whether or not a crossing occurs during the interaction, means that the two-level atom *does not recognize* the presence of a crossing. This provides the reason for referring to this regime as the *nonsubstantial crossing*.

E. Half crossing

In this case, the crossing occurs near the turn-on time T_i or the turn-off time T_f. In other words, one of T_i and T_f is small while the other is large. For simplicity and without loss of generality we will assume that the turn-on time $T_i = -\tau_i < 0$ is far from the crossing and negative and the turn-off time $T_f = \tau_f$ is near the crossing, positive or negative as illustrated in Fig. 1(c). Then we have to use the power-series expansion (A4) for the parabolic cylinder functions with arguments involving τ_f in Eqs. (10–12) and the weak-coupling or the strong-coupling asymptotic expansions for the parabolic cylinder functions with arguments involving τ_i.

1. Weak-coupling asymptotics

It is obtained from Eqs. (12), (A5), and (A6) and reads

$$P_2(\tau_f, -\tau_i) \sim \frac{1}{2}(1 - e^{-\pi\omega^2/2}) - \frac{\omega}{2\tau_i}\sqrt{1 - e^{-\pi\omega^2}}\cos\xi_w(\tau_i)$$

$$+ \omega\tau_f\sqrt{1 - e^{-\pi\omega^2}}\cos\chi$$

(36)

$$(\tau_i \gg 1, \omega, 2\omega\sqrt{e^{\pi\omega^2} - 1}; \omega|\tau_f| \ll 1),$$

where $\xi_w(\tau_i)$ is defined by Eq. (17) and

$$\chi = \frac{\pi}{4} + \arg\Gamma\left(\frac{1}{2} - i\frac{\omega^2}{4}\right) - \arg\Gamma\left(1 - i\frac{\omega^2}{4}\right).$$

(37)

2. Adiabatic-following solution

This is the regime of large coupling. The solution can be obtained from the general result (B3) derived in Appendix B,

$$P_2(\tau_f, -\tau_i) \sim \frac{1}{2} + \frac{\tau_i\tau_f}{2\omega\sqrt{\tau_i^2 + \omega^2}} - \frac{\omega\cos[\xi_a(\tau_f) + \xi_a(\tau_i)]}{2\sqrt{\tau_i^2 + \omega^2}}$$

(38)

$$(\omega \gg 1; \omega|\tau_f| \ll 1),$$

where $\xi_a(\tau_{i,f})$ is given by Eq. (21).

3. Strong-coupling asymptotics

This asymptotics is obtained from Eqs. (12), (A7), and (A13) and is

$$P_2(\tau_f, -\tau_i) \sim \frac{1}{2}\left(1 - e^{-\pi\omega^2/2}\frac{\tau_i}{\sqrt{\tau_i^2 + \omega^2}}\right)$$

$$-\frac{\omega}{2\sqrt{\tau_i^2 + \omega^2}}\sqrt{1 - e^{-\pi\omega^2}}\cos\xi(\tau_i)$$

$$+\frac{1}{2}\omega\tau_f\sqrt{1 - e^{-\pi\omega^2}}\left(1 + \frac{\tau_i}{\sqrt{\tau_i^2 + \omega^2}}\right)\cos\chi$$

$$(39)$$

$$(\tau_i^2 + \omega^2 \gg 1; \omega|\tau_f| \ll 1),$$

where χ is given by Eq. (37). It is readily verified that the strong-coupling asymptotics (39) contains the weak-coupling asymptotics (36) as a particular case in the limit $\tau_i \gg \omega$ and the adiabatic approximation (38) in the limit $\omega \gg 1$, $\tau_f = 0$. In the particular case of a turn-on time at infinity, $T_i = -\tau_i \to -\infty$, and a turn-off time exactly at the crossing, $\tau_f = 0$, Eq. (39) recovers an earlier result found by Carroll and Hioe [9]:

$$P_2(0, -\infty) = \frac{1}{2}(1 - e^{-\pi\omega^2/2}). \qquad (40)$$

It is this particular case that provides the reason for the term *half crossing* adopted by us. For large ω, the excited-state population tends to one-half, which resembles excitation by asymmetric pulses with constant detuning reported recently [19]. The second term on the right-hand side (rhs) of Eq. (39) describes the first-order correction due to the finite turn-on time τ_i. As a function of τ_i, it generates oscillations around the value determined by the first, zeroth-order term. The third term on the rhs of Eq. (39) describes the first-order correction due to the nonzero turn-off time τ_f. In contrast to the second term, the third term is a linear function of τ_f and does not oscillate.

In Fig. 9, the transition probability is plotted as a function of $T_i = -\tau_i$ for $T_f = \tau_f = 0$ and two scaled coupling strengths, $\omega = 0.3$ and 3. Again, the adiabatic-following solution (38) is accurate for large ω but fails for small ω. The weak-coupling asymptotics (36) is good for small ω, but is inaccurate for large ω. The strong-coupling asymptotics (39) fits the exact results very well for any ω.

IV. APPLICATION TO TIME EVOLUTION IN THE ORIGINAL LANDAU-ZENER MODEL

The results obtained in Sec. III provide a possibility to study time-dependent effects by fixing the turn-on time T_i; then considering the transition probability as a function of T_f gives its time evolution. We will consider in more detail the particular case when $T_i \to -\infty$, representing the original LZ model. The transition probability at time $T_f \equiv T$ can be approximated by using the strong-coupling expansions (34), (39), and (32) in three regimes: when T_f is *large and negative*, when T_f is *small*, and when T_f is *large and positive*.

At large and negative time $T < 0$, $|T| \gg 1$, the relevant ap-
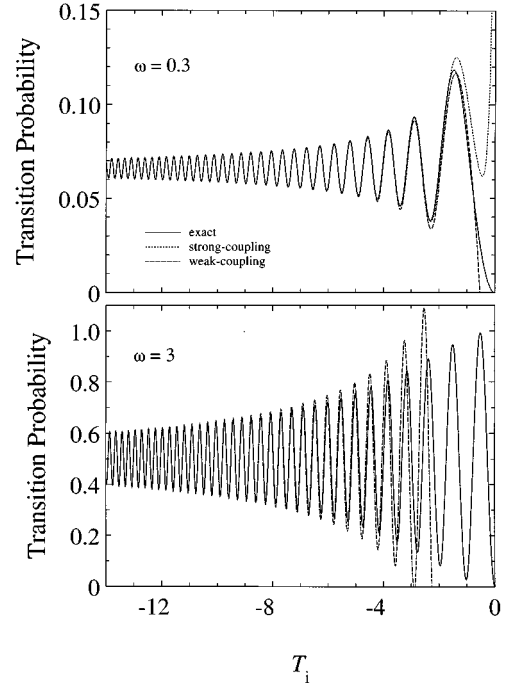
FIG. 9. The transition probability in the case of *half crossing* as a function of the dimensionless turn-on time $T_i = -\tau_i$ for $T_f = 0$ and two scaled coupling strengths, $\omega = 0.3$ and 3. The full curves represent the exact values obtained by numerical integration of Eqs. (1), the long-line dashed curves show the weak-coupling asymptotics (36), and the short-line dashed curves show the strong-coupling asymptotics (39). For $\omega = 0.3$, the adiabatic-following solution (38) is not shown as it gives rather too large values while for $\omega = 3$; the strong-coupling asymptotics and the adiabatic solution are indiscernible from the exact values.

proximation is the no-crossing one (34), which in the limit $T_i \to -\infty$ gives

$$P_2(T, -\infty) \sim \frac{1}{2} + \frac{T}{2\sqrt{T^2 + \omega^2}} \quad (T < 0). \qquad (41)$$

In contrast to the case of a finite turn-on time, there are no oscillations, which shows that they originate from the sudden turn on of the coupling. The transition probability is small and for $|T| \gg \omega, 1$ it tends to $P_2(T, -\infty) \sim \omega^2/4T^2$.

At small time T (near the crossing) regardless of its sign, the transition probability is given by the half-crossing approximation (39), which in the limit $T_i \to -\infty$ reduces to

$$P_2(T, -\infty) \sim \frac{1}{2}(1 - e^{-\pi\omega^2/2}) + \omega T\sqrt{1 - e^{-\pi\omega^2}}\cos\chi(\omega)$$

$$(\omega|T| \ll 1), \quad (42)$$

where χ is given by Eq. (37). At $T = 0$, only the first term on the rhs survives in agreement with (40) while for $T \neq 0$ the transition probability increases linearly with T. Therefore, Eq. (42) gives the correct value and the slope of the transition probability at the crossing point $T = 0$, but a more accu-
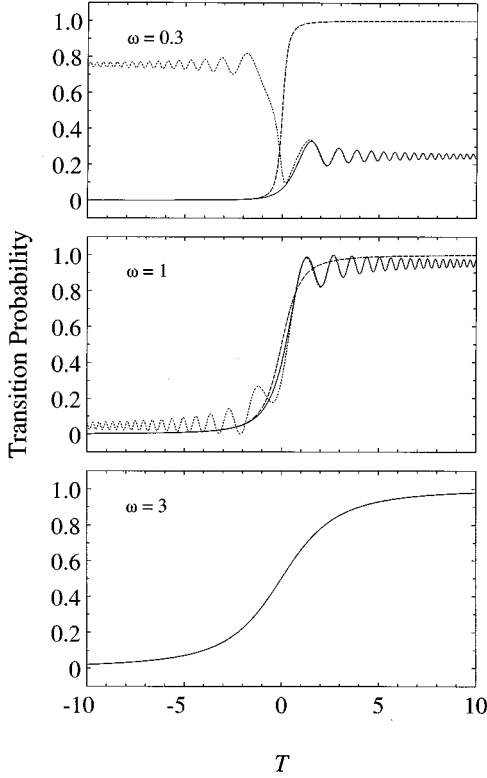
FIG. 10. The time evolution of the transition probability in the original LZ model ($T_i \rightarrow -\infty$) for three scaled coupling strengths, $\omega = 0.3$, 1, and 3. The dimensionless time T is defined by Eq. (4). The full curves represent the exact values, the long-line dashed curves show the no-crossing strong-coupling asymptotics (41), and the short-line dashed curves show the substantial-crossing strong-coupling asymptotics (43). The no-crossing asymptotics is *formally* plotted for $T > 0$, that is, after the crossing; so is the substantial-crossing asymptotics for $T < 0$, that is, before the crossing. For $\omega = 3$ the three curves coincide.

rate approximation in this region requires accounting for more terms in the power series of the parabolic cylinder functions (Appendix C).

At large and positive time $T \gg 1$, that is after the crossing, the transition probability is best approximated by its asymmetric-crossing strong-coupling asymptotics (32), which in the limit $T_i \rightarrow -\infty$ gives

$$
P_2(T, -\infty) \sim \frac{1}{2} + \left(\frac{1}{2} - e^{-\pi\omega^2} \right) \frac{T}{\sqrt{T^2 + \omega^2}}
$$

$$
- e^{-\pi\omega^2/2} \sqrt{1 - e^{-\pi\omega^2}} \frac{\omega \cos\xi(T)}{\sqrt{T^2 + \omega^2}} \quad (T > 0),
$$

$$
(43)
$$

where $\xi(T)$ is given by Eq. (24). The transition probability oscillates irrespective of whether or not the turn-on time T_i is finite. The transition probability is large and for $T \rightarrow \infty$ it tends to the LZ formula (25). In Fig. 10 we compare our analytical approximations (41) and (43) to the exact values for three scaled coupling strengths, $\omega = 0.3$, 1, and 3. The exact values are calculated numerically by the approach de-

scribed in Appendix C. The no-crossing asymptotics (41) is *formally* plotted for $T > 0$, that is, after the crossing; so is the asymmetric-crossing asymptotics (43) for $T < 0$, that is, before the crossing. For $\omega > 1$ they give fairly good approximations in these regions formally forbidden for them. For $\omega < 1$, however, they are only accurate in the regions where they are supposed to be valid, but not outside them.

V. APPLICATION TO SHAPE AND CHIRP EFFECTS

A. The degeneracy of the two-level problem

The results obtained in Sec. III turn out to be very useful in studying the effect of different coupling shapes for the same detuning chirp or the effect of different chirps for the same coupling shape. This is possible because of an interesting but not very widely known peculiarity of the two-level problem: the existence of different pairs of couplings and detunings that give the same transition probability. This can be easily shown in two ways. The first is due to Delos and co-workers [20] who showed that in terms of the new independent variable,

$$
s(t) = \int_0^t \Omega(t')dt', \tag{44}
$$

Eqs. (1) take the simpler form

$$
i\frac{d}{ds}\begin{pmatrix} B_1(s) \\ B_2(s) \end{pmatrix} = \begin{pmatrix} -\Theta(s) & 1 \\ 1 & \Theta(s) \end{pmatrix} \begin{pmatrix} B_1(s) \\ B_2(s) \end{pmatrix}, \tag{45}
$$

where $B_{1,2}(s) = C_{1,2}[t(s)]$ and

$$
\Theta(s) = \frac{\Delta[t(s)]}{\Omega[t(s)]}. \tag{46}
$$

Equations (45) show that in terms of the variable s, the two-level dynamics depends on *one* function $\Theta(s)$ only, called sometimes the Stueckelberg variable. Let us now suppose that the solution for certain $\Delta(t)$ and $\Omega(t)$ is known. Then we can find the function $s(t)$ from (44) and $\Theta(s)$ from (46). Inasmuch as the solution depends on $\Theta(s)$ only, if we replace the particular coupling function $\Omega(t)$ by another function and then find the corresponding detuning $\Delta(t)$ from Eq. (46) using the presumably known $\Theta(s)$, the solution will remain unchanged. All pairs of $\Delta(t)$ and $\Omega(t)$ found in such a way form a *class* of models. This class contains an infinite number of members in which $\Delta(t)$ and $\Omega(t)$ are connected by

$$
\Delta(t) = \Omega(t)\Theta\left(\int_0^t \Omega(t')dt' \right).
$$

We should point out that the populations induced by different pairs are the same only *after* the couplings have turned off. *During* the interaction the populations evolve in different ways because different couplings $\Omega(t)$ lead to different mappings of t onto s.

An alternative though equivalent approach has been used by Hioe and Carroll [21]. They introduce an arbitrary independent variable $z = z(t)$, which is positive, monotonic, and satisfies $z(-\infty) = 0$, $z(+\infty) = 1$. In terms of z, Eqs. (1) become

TABLE I. Various pairs of the couplings and the detunings belonging to the finite Landau-Zener class (47) and the Allen-Eberly class (49). The first two pairs (a) have the same linear chirp, but different coupling shapes; the second pairs (b) have the same hyperbolic-tangent chirp, but different coupling shapes; the third pairs (c) have the same rectangular coupling, but different chirps; the fourth pairs (d) have the same hyperbolic-secant coupling, but different chirps.

Finite Landau-Zener class	Allen-Eberly class
(a) $\Delta_{LZ}(t) = \Delta_{AE}(t) = \beta^2 t$	
$\Omega_{LZ}(t) = \Omega_0 \quad (|t| \leq t_0)$	$\Omega_{AE}(t) = \pi \Omega_0 |t|/(2t_0 \sqrt{e^{(\pi t/2t_0)^2} - 1})$
(b) $\Delta_{LZ}(t) = \Delta_{AE}(t) = (2/\pi)\beta^2 t_0 \tanh(\pi t/2t_0)$	
$\Omega_{LZ}(t) = \Omega_0 \tanh(\pi|t|/2t_0)/\sqrt{2\ln[\cosh(\pi t/2t_0)]}$ $\left[|t| \leq \dfrac{2}{\pi} t_0 \ln(e^{\pi^2/8} + \sqrt{e^{\pi^2/4} - 1})\right]$	$\Omega_{AE}(t) = \Omega_0 \mathrm{sech}(\pi t/2t_0)$
(c) $\Omega_{LZ}(t) = \Omega_{AE}(t) = \Omega_0 \quad (|t| \leq t_0)$	
$\Delta_{LZ}(t) = \beta^2 t$	$\Delta_{AE}(t) = (2/\pi)\beta^2 t_0 \tan(\pi t/2t_0)$
(d) $\Omega_{LZ}(t) = \Omega_{AE}(t) = \Omega_0 \mathrm{sech}(\pi t/2t_0)$	
$\Delta_{LZ}(t) = \beta^2 t_0 [(4/\pi)\tan^{-1}(e^{\pi t/2t_0}) - 1]\mathrm{sech}(\pi t/2t_0)$	$\Delta_{AE}(t) = (2/\pi)\beta^2 t_0 \tanh(\pi t/2t_0)$

$$i\frac{d}{dz}\begin{pmatrix} \widetilde{C}_1(z) \\ \widetilde{C}_2(z) \end{pmatrix} = \begin{pmatrix} -\widetilde{\Delta}(z) & \widetilde{\Omega}(z) \\ \widetilde{\Omega}(z) & \widetilde{\Delta}(z) \end{pmatrix} \begin{pmatrix} \widetilde{C}_1(z) \\ \widetilde{C}_2(z) \end{pmatrix},$$

where $\widetilde{\Omega}(z) = \Omega[t(z)]/\dot{z}$, $\widetilde{\Delta}(z) = \Delta[t(z)]/\dot{z}$, and $\widetilde{C}_{1,2}(z) = C_{1,2}[t(z)]$. If the solution for certain $\Delta(t)$ and $\Omega(t)$ is known we can choose an appropriate function $z(t)$ [its choice does not have to be related to $\Delta(t)$ and $\Omega(t)$ and is a matter of convenience] and then, we can find the functions $\widetilde{\Omega}(z)$ and $\widetilde{\Delta}(z)$, which define the class. From these generating functions we can find the other members of the class by choosing various functions $z(t)$. Since the number of the auxiliary functions $z(t)$ is infinite, the number of pairs in the class is infinite too.

The generalization of the LZ model for a finite coupling duration, considered in the previous section, belongs to a class of models as well. For simplicity, we will only consider the case of symmetric crossing (Sec. III A) when $T_i = -\tau$, $T_f = \tau$. In terms of the variable s, this class is readily verified to have a very simple definition

$$\Theta(s) = \frac{s}{\omega^2} \quad (|s| \leq \omega\tau). \tag{47}$$

In contrast to the rather simple time dependence of $\Delta(t)$ and $\Omega(t)$ in the finite LZ model (3), the class (47) contains a number of pairs in which $\Delta(t)$ and $\Omega(t)$ are smooth functions of time. For example, such a pair is the last one in Table I and in Fig. 11 below.

There are several classes of analytically solvable models that can be obtained from the exact solutions listed, e.g., in Refs. [22] and [23]. We can find similar pairs in different classes in which either the coupling $\Omega(t)$ or the detuning $\Delta(t)$ is the same. There are, however, some limitations. For example, if the detuning $\Delta(t)$ of a given pair in a class changes sign, say at $t=0$, then $\Theta(0)=0$ and the detunings of all pairs in the same class should change sign at $t=0$ as well. Also, if the "pulse area" for a certain member of the class is infinite (as in the original LZ model) then it is infinite for any other member too. The requirement that the detuning passes through resonance at $t=0$ limits the number of classes that can be compared to the LZ class (47) to just two: the Nikitin class [18] and the Allen-Eberly class [12]. We choose the latter, which provides the transition probability in terms of elementary functions while in the Nikitin class it is given in terms of confluent hypergeometric functions [18].
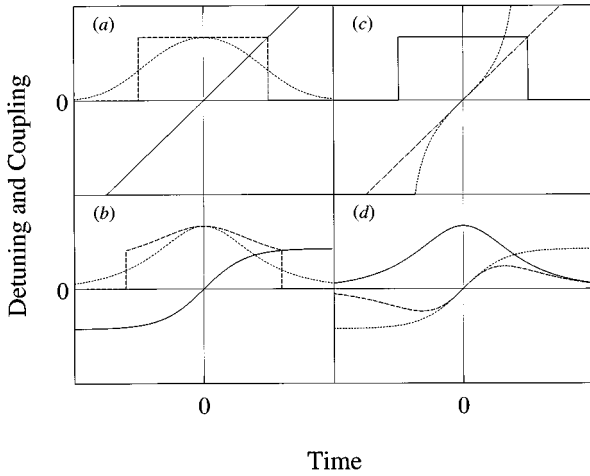
FIG. 11. Plot of the couplings and the detunings from Table I. Throughout, a long-line dashed curve shows a quantity belonging to the finite LZ class, while a short-line dashed curve shows a quantity belonging to the Allen-Eberly class; a full line shows a quantity that is the same for both classes. (a) The same linear chirp, different coupling shapes; (b) the same hyperbolic-tangent chirp, different coupling shapes; (c) the same rectangular coupling, different chirps; (d) the same hyperbolic-secant coupling, different chirps.

B. Shape and chirp effects

Demkov and Kunicke were the first who solved (in a little known paper [7,11,23]) the model that was later treated by a number of authors. A particular case of this model was later solved independently by Allen and Eberly [12]. It is this particular case (referred to hereafter as AE) that we are going to consider. It is defined by

$$\Omega(t)=\Omega_0 \mathrm{sech}\frac{\pi t}{2t_0}, \quad \Delta(t)=\frac{2\beta^2 t_0}{\pi}\tanh\frac{\pi t}{2t_0} \quad (48)$$

and the corresponding class is defined in terms of the variable s (44) by

$$\Theta(s)=\frac{2\tau}{\pi\omega}\tan\frac{\pi s}{2\omega\tau} \quad (|s|\leq\omega\tau), \quad (49)$$

where $\omega=\Omega_0/\beta$, $\tau=\beta t_0$. The transition probability at $t\rightarrow+\infty$ for a two-level system, initially in its ground state at $t\rightarrow-\infty$, is given by

$$P_2=1-\mathrm{sech}^2\frac{4\tau^2}{\pi}\cos^2\left[2\tau\sqrt{\omega^2-\frac{4\tau^2}{\pi^2}}\right]. \quad (50)$$

For $\omega<2\tau/\pi$ the cosine is to be replaced by a hyperbolic cosine. The reason for the way in which the parameters of the AE model (48) are written is to allow comparison with the finite LZ model (3) studied in the preceding sections: the maximum coupling strength Ω_0, the pulse area $2\Omega_0 t_0$, and the detuning slope β^2 at the crossing are the same for the AE model and the finite LZ model.

In Table I, we have compared members of the finite LZ class to members of the AE class in four cases. They are shown schematically in Fig. 11. Case (a) both in Table I and in Fig. 11 shows pairs with *the same linear detuning chirp*
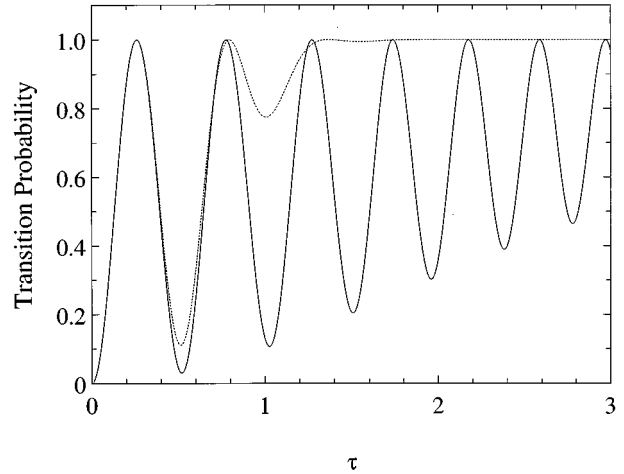
FIG. 12. The transition probabilities for the finite Landau-Zener class (full curve) and the Allen-Eberly class (dashed curve) plotted as functions of the dimensionless parameter τ for $\omega=3$.

but different couplings. Case (b) shows pairs with *the same hyperbolic-tangent detuning chirp* but different couplings. Case (c) shows pairs with *the same rectangular coupling* but different detuning chirps. Case (d) shows pairs with *the same hyperbolic-secant coupling* but different detuning chirps.

In Fig. 12, we compare the transition probabilities for the finite LZ class and the AE class plotted as functions of τ for $\omega=3$. In Fig. 13, we compare the transition probabilities as functions of ω for $\tau=1$. It is seen that the models in the LZ class generate oscillations with much larger amplitudes. On the one hand, for the models with the same detuning [cases (a) and (b)] this fact can be explained as due to the sudden changes undergone by the system at the turn-on and the turn-off times of the coupling for the models in the LZ class. In other words, the models in the AE class are much more adiabatic. On the other hand, for the models with the same coupling [cases (c) and (d)], this feature comes from the fact that the system spends a longer time near resonance (that is
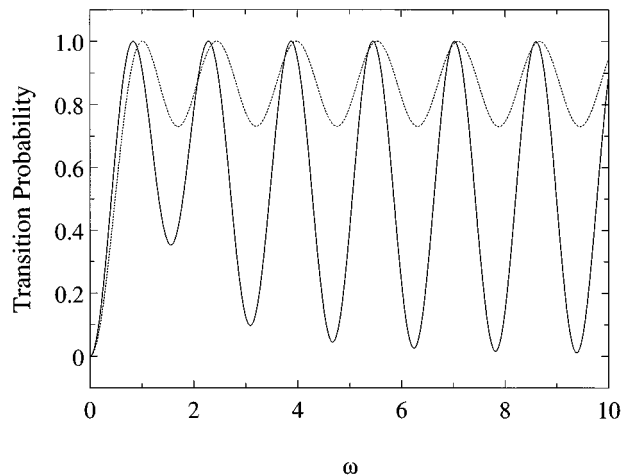
FIG. 13. The transition probabilities for the finite Landau-Zener class (full curve) and the Allen-Eberly class (dashed curve) plotted as functions of the dimensionless coupling strength ω for $\tau=1$.

the detuning increases more slowly) for the LZ models than for the AE models. Cases (c) and (d) also show that oscillations can be generated not only by a sudden turn-on or turn-off of the interaction but also if the external field is near resonance with the system for a sufficiently long time.

VI. SUMMARY OF THE RESULTS AND CONCLUSIONS

We have presented the generalization of the Landau-Zener model for a constant coupling of a *finite* duration. The exact evolution matrix has been expressed in terms of sums of by-products of the parabolic cylinder function $D_\nu(z)$ estimated at the scaled turn-on time T_i and at the turn-off time T_f. Several approximations in terms of simpler functions have been derived based on (i) the large-argument asymptotics of $D_\nu(z)$ corresponding to large T_i and T_f and weak coupling; (ii) the large-argument and large-order asymptotics of $D_\nu(z)$ corresponding to large T_i and T_f and strong coupling; (iii) the power-series expansion of $D_\nu(z)$ corresponding to small T_i and T_f; (iv) the adiabatic-following solution corresponding to large coupling irrespective of T_i and T_f. These approximations have been applied to several physically distinct cases. The most important of them is the case of *substantial crossing* in which the crossing occurs during the interaction and both T_i and T_f are far from the crossing. A particular case of this is the symmetric crossing when $T_i = -T_f$. It is the straightforward generalization of the standard LZ model and provides the correction for a finite coupling duration. The case of nonsymmetric T_i and T_f demonstrates the effect of adding a constant detuning that displaces the crossing point. Comparison of the substantial-crossing case with the case of *no crossing*, when the detuning is a linear function of time but is far from resonance, so that a crossing does not occur during the interaction, demonstrates explicitly the importance of level crossing in quantum physics. Namely, the transition probability is much larger in the former case for otherwise equal parameters (coupling strength, coupling duration, detuning slope). Furthermore, a different physical situation arises in the case of the *nonsubstantial crossing*, when both T_i and T_f are near the crossing: then up to the fourth order in T_f and T_i the transition probability depends on the time duration only rather than on the presence or the absence of a level crossing. Finally, the last analytically treated case is that of the *half crossing*, when T_i is far from the crossing while T_f is near the crossing. Then in the adiabatic limit the transition probability tends to one-half rather than to unity as for the substantial crossing. It has been shown that in all approximations are the cases (except for nonsubstantial crossing), the adiabatic approximations are very precise for large ω, irrespective of where the turn-on and the turn-off times are. The weak-coupling asymptotics is accurate for turn-on and turn-off times far from the crossing and much larger than the scaled coupling strength ω. The strong-coupling asymptotics are valid when ω and/or $T_{i,f}$ are large, which means that it contains the adiabatic approximation and the weak-coupling asymptotics as particular cases.

The strong-coupling asymptotics for no crossing, half crossing, and asymmetric substantial crossing have been applied to study the time dependence in the original LZ model when the coupling is turned on at $-\infty$. It has been shown

that the no-crossing approximation provides a very good fit to the exact values for negative times and the substantial-crossing approximation is very accurate for positive times. Near crossing, it is the half-crossing approximation that describes most accurately the time evolution. The exact time evolution of the transition probability has been calculated numerically by a new algorithm, presented in Appendix C, which can be useful in other related studies on coherent excitation.

The finite LZ model has been compared to the Allen-Eberly model. Comparison has been facilitated by the degeneracy of the two-level problem, which results in the fact that the same transition probability is obtained not only for a single model but for a *class* of models. The classes generated by the finite Landau-Zener model and the Allen-Eberly model contain members with the same coupling but different detuning chirps as well as members with the same chirp but different couplings. The former pairs show chirp effects while the latter pairs demonstrate pulse-shape effects.

Finally, the results reported in this paper can be used to model the interaction dynamics near the crossing in any level-crossing problem whenever the finite transition time is to be accounted for. In a forthcoming paper, some of the results, obtained in this work for a single level crossing, are applied to multiple level crossings, a case encountered in coherent interaction of atoms and molecules with frequency modulated light.

APPENDIX A: RELEVANT PROPERTIES OF THE PARABOLIC CYLINDER FUNCTION

The parabolic cylinder (Weber) function $D_\nu(z)$ [13] is a solution of the Weber equation

$$\frac{d^2}{dz^2}D_\nu(z)+\left(\nu+\frac{1}{2}-\frac{1}{4}z^2\right)D_\nu(z)=0. \quad \text{(A1)}$$

It has the derivative property

$$\frac{d}{dz}[e^{z^2/4}D_\nu(z)]=\nu e^{z^2/4}D_{\nu-1}(z) \quad \text{(A2)}$$

and satisfies the Wronskian relation

$$W\{D_\nu(z),D_\nu(-z)\}\equiv D_\nu(z)\frac{d}{dz}D_\nu(-z)-D_\nu(-z)\frac{d}{dz}D_\nu(z)$$

$$=\frac{\sqrt{2\pi}}{\Gamma(-\nu)}. \quad \text{(A3)}$$

We can simplify the exact results (10)–(12) when the scaled turn-on time T_i and the turn-off time T_f are small or large compared to unity. In these cases we have used the approximations to the parabolic cylinder functions listed below.

1. Power-series expansion

This expansion is convenient for small T_i or T_f and has the form [24]

$$D_\nu(z) = 2^{\nu/2}\pi^{1/2}e^{z^2/4}\sum_{n=0}^{\infty}\frac{(-z\sqrt{2})^n}{n!\,\Gamma\!\left[\frac{1}{2}(1-n-\nu)\right]}. \quad (A4)$$

2. Large-argument asymptotic expansions

These expansions are convenient when T_i or T_f are much larger than unity *and* ω and have the form [13]

$$D_\nu(z) \sim z^\nu e^{-z^2/4}$$

$$\times\left[\sum_{n=0}^{N}\frac{\left(-\frac{1}{2}\nu\right)_n\left(\frac{1}{2}-\frac{1}{2}\nu\right)_n}{n!\left(-\frac{1}{2}z^2\right)_n}+O(|z^2|^{-N-1})\right]$$

$$(A5)$$

$$\left(|\arg z|<\frac{3\pi}{4}, \quad \nu \text{ fixed}, \quad |z|\to\infty\right),$$

where $(a)_n = \Gamma(a+n)/\Gamma(a)$. To find the asymptotics for other values of $\arg z$ of the parabolic cylinder functions involved in Eqs. (10)–(12) we can make use of the connection formula [13]

$$D_\nu(z) = e^{i\pi\nu}D_\nu(-z)+\frac{\sqrt{2\pi}}{\Gamma(-\nu)}e^{(i\nu+1)\pi/2}D_{-1-\nu}(-iz). \quad (A6)$$

The existence of different asymptotic expansions for different values of $\arg z$ is merely a manifestation of the Stokes phenomenon [16,17].

3. Large-argument and large-order asymptotics

These expansions are convenient when the turn-on time T_i or the turn-off time T_f and the scaled coupling strength ω are simultaneously much larger than unity. These expansions are much more complicated than the weak-coupling asymptotics (A5). For the particular functions involved in Eqs. (10)–(12) with phases of the arguments equal to $\pi/4$ the asymptotic expansions can be derived from the general results of Olver [25] and their leading terms are

$$D_{i\omega^2/2}(\tau\sqrt{2}e^{-i\pi/4}) \sim \cos\vartheta(\tau)e^{\pi\omega^2/8+i\eta}, \quad (A7)$$

$$D_{-i\omega^2/2}(\tau\sqrt{2}e^{i\pi/4}) \sim \cos\vartheta(\tau)e^{\pi\omega^2/8-i\eta}, \quad (A8)$$

$$D_{-1-i\omega^2/2}(\tau\sqrt{2}e^{i\pi/4}) \sim \frac{\sqrt{2}}{\omega}\sin\vartheta(\tau)e^{\pi\omega^2/8-i\eta-i\pi/4}, \quad (A9)$$

$$D_{-1+i\omega^2/2}(\tau\sqrt{2}e^{-i\pi/4}) \sim \frac{\sqrt{2}}{\omega}\sin\vartheta(\tau)e^{\pi\omega^2/8+i\eta+i\pi/4} \quad (A10)$$

$$(\tau,\omega\to\infty, \tau/\omega \text{ is arbitrary})$$

where

$$a\,\eta = -\frac{\omega^2}{4}+\frac{\omega^2}{2}\ln\left[\frac{1}{\sqrt{2}}(\tau+\sqrt{\tau^2+\omega^2})\right]+\frac{\tau}{2}\sqrt{\tau^2+\omega^2}, \quad (A11)$$

$$a\cos\vartheta(\tau) = \sqrt{\frac{1}{2}\left(1+\frac{\tau}{\sqrt{\tau^2+\omega^2}}\right)},$$

$$a\sin\vartheta(\tau) = \sqrt{\frac{1}{2}\left(1-\frac{\tau}{\sqrt{\tau^2+\omega^2}}\right)} \quad (A12)$$

and τ and ω are assumed positive. The parameter ϑ is exactly the angle of the rotation connecting the diabatic and the adiabatic bases (see Appendix B). For functions with a phase of the argument equal to $3\pi/4$, the large-order and large-argument asymptotics can be obtained from Eqs. (A7)–(A10) by using the connection formula (A6) and are given by

$$aD_{i\omega^2/2}(\tau\sqrt{2}e^{i3\pi/4}) \sim \cos\vartheta(\tau)e^{-3\pi\omega^2/8+i\eta}$$

$$+\frac{\omega\sqrt{\pi}}{\Gamma\!\left(1-\frac{1}{2}i\omega^2\right)}\sin\vartheta(\tau)$$

$$\times e^{-\pi\omega^2/8-i\eta-i\pi/4}, \quad (A13)$$

$$aD_{-1+i\omega^2/2}(\tau\sqrt{2}e^{i3\pi/4})$$

$$\sim \frac{\sqrt{2}}{\omega}\sin\vartheta(\tau)e^{-3\pi\omega^2/8+i\eta-i3\pi/4}$$

$$+\frac{\sqrt{2\pi}}{\Gamma\!\left(1-\frac{1}{2}i\omega^2\right)}\cos\vartheta(\tau)e^{-\pi\omega^2/8-i\eta}$$

$$(A14)$$

$$(\tau,\omega\to\infty, \tau/\omega \text{ is arbitrary}).$$

APPENDIX B: ADIABATIC-FOLLOWING SOLUTION

The adiabatic solution can be obtained by transforming Eqs. (1) into the adiabatic representation by the unitary transformation

$$\mathbf{C}(T) = \mathbf{R}(T)\mathbf{A}(T),$$

where

$$\mathbf{R}(T) = \begin{pmatrix} \cos\vartheta(T) & \sin\vartheta(T) \\ -\sin\vartheta(T) & \cos\vartheta(T) \end{pmatrix},$$

$$\tan 2\,\vartheta(T) = \frac{\Omega(T)}{\Delta(T)} = \frac{\omega}{T}. \tag{B1}$$

The Schrödinger equation in the adiabatic representation has the form

$$i\mathbf{A}' = \begin{pmatrix} -\sqrt{\Omega^2 + \Delta^2} & -i\,\vartheta' \\ i\,\vartheta' & \sqrt{\Omega^2 + \Delta^2} \end{pmatrix} \mathbf{A},$$

where the primes mean differentiation with respect to T. By definition, the system evolves adiabatically if it remains in the same adiabatic state; this happens with a large probability if the adiabatic condition

$$|\vartheta'| \ll \sqrt{\Omega^2 + \Delta^2} \tag{B2}$$

is satisfied. Then it is readily shown that the adiabatic amplitudes evolve as

$$\mathbf{A}(T_f) = \mathbf{U}_a(T_f, T_i)\mathbf{A}(T_i),$$

$$\mathbf{U}_a(T_f, T_i) = \begin{pmatrix} e^{i\zeta_a(T_f, T_i)} & 0 \\ 0 & e^{-i\zeta_a(T_f, T_i)} \end{pmatrix},$$

where

$$\zeta_a(T_f, T_i) = \int_{T_i}^{T_f} \sqrt{\Omega^2(T) + \Delta^2(T)}\, dT$$

is the adiabatic phase. The evolution matrix in the original diabatic representation is

$$\mathbf{U}(T_f, T_i) = \mathbf{R}(T_f)\mathbf{U}_a(T_f, T_i)\mathbf{R}^T(T_i).$$

Thus, we find the adiabatic-following solution for the transition probability $P_2(T_f, T_i) = |U_{21}(T_f, T_i)|^2$,

$$P_2(T_f, T_i) \approx \frac{1}{2} - \frac{T_i T_f}{2\sqrt{(T_i^2 + \omega^2)(T_f^2 + \omega^2)}}$$

$$- \frac{\omega^2}{2\sqrt{(T_i^2 + \omega^2)(T_f^2 + \omega^2)}}\cos 2\,\zeta_a(T_f, T_i), \tag{B3}$$

where

$$\zeta_a(T_f, T_i) = \int_{T_i}^{T_f} \sqrt{T^2 + \omega^2}\, dT$$

$$= \frac{1}{2}(T_f\sqrt{T_f^2 + \omega^2} - T_i\sqrt{T_i^2 + \omega^2})$$

$$+ \frac{\omega^2}{2}\ln\frac{T_f + \sqrt{T_f^2 + \omega^2}}{T_i + \sqrt{T_i^2 + \omega^2}}$$

$$= \frac{1}{2}[\xi_a(T_f) - \xi_a(T_i)] \tag{B4}$$

with $\xi_a(T)$ defined by (21).

APPENDIX C: NUMERICAL INTEGRATION OF THE LANDAU-ZENER PROBLEM

The numerical integration of the two-state equations (1) for the original LZ model (2) is not a trivial problem because the coupling does not vanish at infinity and the detuning goes to infinity too slowly. The straightforward way of integrating Eqs. (1) is to start at a certain large negative time and propagate the solution towards $t \to +\infty$. Starting at a finite time, however, generates spurious oscillations in the solution as can be seen from Eqs. (32) and (34). Certainly, their amplitude decreases when one moves the start-up time towards $t \to -\infty$ but nonetheless, they are always present although they can be made invisible in a figure. Furthermore, this procedure requires large computational time. To a great extent this can be remedied by choosing the initial state, at "large" finite time, to be the adiabatic state at that instant. We know that far away from the crossing region the adiabatic state is a good approximation to the real solution, and the numerical integration proceeds without oscillations until we approach the nonadiabatic region. However, we propose here an alternative, rigorous, and much more efficient solution to this problem. The method is based on three key points: (i) we start the integration at $t = 0$ and propagate the solution towards the desired time; (ii) we solve the equation for the population inversion rather than Eqs. (1); (iii) we find the initial conditions at $t = 0$ by using the dependence of the half-crossing transition probability (42) on the turn-off time.

To find the equation for the population inversion we apply the Feynman-Vernon-Hellwarth transformation [26]

$$U = C_1 C_2^* + C_1^* C_2,$$

$$V = -i(C_1 C_2^* - C_1^* C_2),$$

$$W = C_2 C_2^* - C_1 C_1^*$$

to Eqs. (1) and obtain the well-known optical Bloch equations

$$\frac{d}{dT}\begin{pmatrix} U \\ V \\ W \end{pmatrix} = 2\begin{pmatrix} 0 & -T & 0 \\ T & 0 & -\omega \\ 0 & \omega & 0 \end{pmatrix}\begin{pmatrix} U \\ V \\ W \end{pmatrix}.$$

By repeated differentiation we can decouple these equations to obtain the following third-order differential equation for the population inversion W:

$$TW''' - W'' + 4T(\omega^2 + T^2)W' - 4\omega^2 W = 0.$$

The numerical integration of this equation by a standard fourth-order Runge-Kutta algorithm requires the values of up to the third derivative of W at $T = 0$. They can be found by

keeping more terms in the half-crossing equation (42),

$$P_2(T, -\infty) = \frac{1}{2}(1 - e^{-\pi\omega^2/2}) + \omega T \sqrt{1 - e^{-\pi\omega^2}} \cos\chi$$

$$+ \omega^2 T^2 e^{-\pi\omega^2/2} + \frac{1}{3}\omega T^3$$

$$\times (\sin\chi - 2\omega^2\cos\chi)\sqrt{1 - e^{-\pi\omega^2}} + \cdots,$$

where $\chi(\omega)$ is given by (37). This is in fact the Taylor expansion of the transition probability versus T. We can therefore identify the initial values of the derivatives of $W(T) = 2P_2(T, -\infty) - 1$ as

$$W(0) = -e^{-\pi\omega^2/2},$$

$$W'(0) = 2\omega\sqrt{1 - e^{-\pi\omega^2}}\cos\chi,$$

$$W''(0) = 4\omega^2 e^{-\pi\omega^2/2},$$

$$W'''(0) = 4\omega(\sin\chi - 2\omega^2\cos\chi)\sqrt{1 - e^{-\pi\omega^2}}.$$

We should also note that the exact values of the transition probability can be found from Eq. (12) by taking the asymptotic limits of the parabolic cylinder functions at $-\infty$ and calculating their values at time T_f by using power series, integral representations, or asymptotic series. This, however, does not represent a more efficient approach than that described above.

[1] I.I. Rabi, Phys. Rev. **51**, 652 (1937).

[2] L.D. Landau, Phys. Z. Sowjetunion **2**, 46 (1932); C. Zener, Proc. R. Soc. London A **137**, 696 (1932).

[3] P. Ao and J. Rammer, Phys. Rev. Lett. **62**, 3004 (1989); V.M. Akulin and W.P. Schleich, Phys. Rev. A **46**, 4110 (1992).

[4] V.N. Ostrovsky, J. Phys. B **24**, 4553 (1991).

[5] C.Y. Zhu and H. Nakamura, J. Chem. Phys. **97**, 8497 (1992); **101**, 4855 (1994).

[6] K.-A. Suominen, Opt. Commun. **93**, 126 (1992).

[7] K.-A. Suominen and B.M. Garraway, Phys. Rev. A **45**, 374 (1992).

[8] B.M. Garraway and S. Stenholm, Phys. Rev. A **45**, 364 (1992).

[9] C.E. Carroll and F.T. Hioe, J. Opt. Soc. Am. B **2**, 1355 (1985); J. Phys. A **19**, 1151 (1986); **19**, 2061 (1986).

[10] D. Bouwmeester, N.H. Dekker, F.E.v. Dorselaer, C.A. Schrama, P.M. Visser, and J.P. Woerdman, Phys. Rev. A **51**, 646 (1995).

[11] Yu.N. Demkov and M. Kunicke, Vest. Leningr. Univ. Fiz. Khim. **16**, 39 (1969).

[12] L. Allen and J.H. Eberly, *Optical Resonance and Two-Level Atoms* (Wiley, New York, 1975).

[13] A. Erdélyi, W. Magnus, F. Oberhettinger, and F.G. Tricomi, *Higher Transcendental Functions* (McGraw-Hill, New York, 1953), Vol. II.

[14] *Handbook of Mathematical Functions*, edited by M. Abramowitz and I.A. Stegun (Dover, New York, 1964).

[15] K. Mullen, E. Ben-Jacob, Y. Gefen, and Z. Schuss, Phys. Rev. Lett. **62**, 2543 (1989).

[16] R.B. Dingle, *Asymptotic Expansions: Their Derivation and Interpretation* (Academic, London, 1973).

[17] F.W.J. Olver, *Asymptotics and Special Functions* (Academic, London, 1974).

[18] N.V. Vitanov, J. Phys. B **27**, 1791 (1994).

[19] N.V. Vitanov and P.L. Knight, J. Phys. B **28**, 1905 (1995).

[20] J.B. Delos and W.R. Thorson, Phys. Rev. A **6**, 728 (1972); T.R. Dinterman and J.B. Delos, *ibid.* **15**, 463 (1977).

[21] F.T. Hioe and C.E. Carroll, Phys. Rev. A **32**, 1541 (1985); J. Phys. A **19**, 3579 (1986).

[22] B.W. Shore, *The Theory of Coherent Atomic Excitation*, Vol. I (Wiley, New York, 1990).

[23] B.M. Garraway and K.-A. Suominen, Rep. Prog. Phys. **58**, 365 (1995).

[24] K.M. Abadir, J. Phys. A **26**, 4059 (1993).

[25] F.W.J. Olver, J. Res. Natl. Bur. Stand. **63B**, 131 (1959).

[26] R.P. Feynman, F.L. Vernon, and R.W. Hellwarth, J. Appl. Phys. **28**, 49 (1957).